Physics

Physics fields

Okayama University   *Year* 2007

Hydrophobic effect in the pressure-temperature plane

Kenichiro Koga
Okayama University, koga@cc.okayama-u.ac.jp

Hydrophobic effect in the pressure-temperature plane

Kenichiro Koga

Department of Chemistry, Faculty of Science, Okayama University, Tsushima-Naka 3-1-1, Okayama 700-8530, Japan

The free energy of the hydrophobic hydration and the strength of the solvent-mediated attraction between hydrophobic solute molecules are calculated in the pressure-temperature plane. This is done in the framework of an exactly soluble model that is an extension of the lattice model proposed by Kolomeisky and Widom [A. B. Kolomeisky and B. Widom, Faraday Discuss. **112**, 81 (1999)]. The model takes into account both the mechanism of the hydrophobic effect dominant at low temperatures and the opposite mechanism of solvation appearing at high temperatures and has the pressure as a second thermodynamic variable. With this model, two boundaries are identified in the pressure-temperature plane: the first one within which the solubility, or the Ostwald absorption coefficient, decreases with increasing temperature at fixed pressure and the second one within which the strength of solvent-mediated attraction increases with increasing temperature. The two are nearly linear and parallel to each other, and the second boundary lies in the low-temperature and low-pressure side of the first boundary. It is found that a single, near-linear relation between the hydration free energy and the strength of the hydrophobic attraction holds over the entire area within the second boundary in the pressure-temperature plane. © *2004 American Institute of Physics.*
[DOI: 10.1063/1.1792571]

I. INTRODUCTION

The fact that hydrophobes dissolve very little in water tells us an associated free energy change due to the accommodation of a hydrophobic molecule in water being positive; but the essential feature of the hydrophobic effect manifests itself in the fact that the low solubility becomes even lower with increasing temperature.[1,2] The decreasing solubility with increasing temperature means that the change in enthalpy and the relevant part of the change in entropy accompanying the transfer of a hydrophobic molecule into water are both negative. This in turn means that the unfavorable entropic contribution to the free energy (a positive value) exceeds the favorable energetic contribution, for the associated free energy change is positive.[3] The unfavorable free change arises because structure of solvent molecules is more ordered (so has a smaller entropy) around each solute molecule than elsewhere.

But if the temperature is further increased, and if the boiling point of water at a given pressure does not intervene, the solubility reaches its minimum and then turns to increase. The thermodynamic properties at such higher temperatures are no longer those characteristic of the hydrophobic effect: the associated free energy change is still positive, but it is because an unfavorable energy change exceeds a favorable associated entropy change. This means that structure of solvent molecules is less ordered (so has a larger entropy) around each solute than elsewhere. Thus, the temperature of the solubility minimum, i.e., the point at which a solute is most hydrophobic, is actually a characteristic temperature around which the hydrophobic hydration is being overcome by the opposite mechanism of solvation.

There is another characteristic temperature of the hydro-phobic effect for each given system: the temperature at which the solvent-mediated attraction between pairs of hydrophobic molecules is strongest. Below that temperature the attraction is due to the hydrophobic effect (the solvation of two solute molecules is entropically less unfavorable when the two are close together than when they are far apart) whereas above that temperature it is due to the opposite mechanism (a favorable energy difference overweighs an unfavorable entropy difference). Thus the mechanism of attraction changes around this second characteristic temperature. Identifying this temperature would be one important step to understand the temperature effect on the stability of proteins.[4–7]

The relevant part of the free energy of transfer is insensitive to the pressure to moderate pressures (Henry's law or the invariance of the partition coefficient of solutes). So the temperature dependence of the free energy and the characteristic temperatures of the hydrophobic effect, too, are insensitive to pressure. But we may not anticipate they continue to be so with increasing pressure above moderate pressures because then the structure of solvent changes significantly. There are numerous studies, both experimental and theoretical, on the hydrophobic effect so that even representative works cannot be cited here all.[8–25] Many of the theoretical studies are based on realistic models of water,[10,12,14,16–22] some focusing on the origin of solubility minimum[14,16] and some addressing pressure effects on the hydrophobic interaction in connection with pressure denaturation of proteins.[13,18,20,21] We will calculate, with a lattice model to be described below, the characteristic temperatures of the hydrophobic hydration and the hydrophobic attraction as functions of pressure. We notice that more realistic models can provide far more detailed account on the hydrophobic

effect. Our aim here is to reveal, in the pressure-temperature space, some general consequences arising from the essential mechanism of the hydrophobic effect alone, which, we hope, are independent of models and best studied by a simple model.

Since both the hydrophobic hydration and the hydrophobic attraction result from the entropically unfavorable structural changes in the solvent around each solute molecule,[2,26] it is reasonable to anticipate some connection between the hydration free energy and the strength of the hydrophobic attraction. Our previous study[27] of a lattice model of the hydrophobic attraction[28] (the origin of the model to be described below) showed that the hydration free energy of a single solute and the magnitude of the solvent-mediated attraction between the two solutes, both divided by kT, are linearly correlated with each other. The results were obtained from exact calculations for the one-dimensional model and virtually exact calculations (Monte Carlo simulation) for the three-dimensional model. Subsequently, we also found that the Bethe-Guggenheim approximation with the coordination number $Z=2$, 3, 8, and ∞ ($Z=2$ is the one-dimensional model and $Z=\infty$ the mean-field approximation) gives linear relationships nearly parallel to each other.[29] We will examine whether or not the linear relation between the hydration free energy and the magnitude of the solvent-mediated potential of mean force is found for the present model and, if it is found, identify how far the linear relation persists in the pressure-temperature plane.

In the following section we will briefly summarize the thermodynamics relevant to the hydrophobic effect and then define the characteristic temperatures. In Sec. III, we will introduce the lattice model with which we calculate the thermodynamic properties and the solvent-mediated potential of mean force. Numerical results are displayed in Sec. IV. The main results are summarized in the concluding Sec. V.

II. THERMODYNAMICS OF THE HYDROPHOBIC EFFECT

We consider here thermodynamics for transferring a molecule A from a phase α to a phase β under the condition that the temperature T and the pressure P of each phase *separately* are the same before and after the transfer. More general accounts on the thermodynamics of transfer are found, for example, in our earlier paper.[29]

Let μ^α and μ^β be the chemical potentials of A in the phase α and β. Then the change ΔG in the composite system's Gibbs free energy is $\mu^\beta - \mu^\alpha$, and the part ΔG^* of ΔG which is relevant to hydrophobic hydration is

$$\Delta G^* = \Delta G - kT \ln(\rho^\beta/\rho^\alpha), \tag{1}$$

where k is Boltzmann's constant and ρ^α and ρ^β are the number densities of A in the phases α and β. If either phase is dilute in A, the whole of the dependence of ΔG on the concentration of A in that phase is canceled with the second term in Eq. (1), and the resulting ΔG^* is then independent of that concentration.

The corresponding change ΔS in the entropy of the composite system has, too, a logarithmic dependence on ρ^α or ρ^β if the phase α or β is dilute in A, and so the part of ΔS defined by

$$\Delta S^* = \Delta S + k \ln(\rho^\beta/\rho^\alpha) \tag{2}$$

is independent of the concentration of the phase dilute in A. Let ϵ^α and ϵ^β be the coefficients of thermal expansion of the two phases. Then from Eq. (1)

$$\Delta S^* = -\frac{\partial \Delta G^*}{\partial T} + kT(\epsilon^\beta - \epsilon^\alpha), \tag{3}$$

the temperature differentiation being at fixed pressure and fixed composition of each phase. (The pressures of α and β need not to be the same.) The change in the enthalpy of the composite system is

$$\Delta H = \Delta G + T\Delta S = \Delta G^* + T\Delta S^*, \tag{4}$$

and is given in terms of a derivative of ΔG^*:

$$\Delta H = \frac{\partial \Delta G^*/T}{\partial 1/T} + kT^2(\epsilon^\beta - \epsilon^\alpha). \tag{5}$$

When the two phases are in equilibrium with respect to the transfer of A, $\Delta G = \mu^\beta - \mu^\alpha = 0$, and so

$$\Delta G^* = -kT \ln \Sigma, \tag{6}$$

where

$$\Sigma = (\rho^\beta/\rho^\alpha)_{\text{eq}}. \tag{7}$$

Since this ratio of the number densities, or the partition coefficient, is accessible by experiments, Eq. (6) with Eq. (7) provides a route from experiments to the thermodynamic quantities of transfer relevant to solvation. Furthermore, there are three common cases in which ΔG^* and its derivatives are practically functions of temperature alone, independent of the concentrations of A in both phases, and independent of whether or not the two phases are in equilibrium with respect to the transfer of the A molecule. The first is when β is a condensed phase dilute in A and α is a dilute gas. Then Σ is the Ostwald absorption coefficient, which is in this case a function of temperature alone. The second is when α and β are both condensed phases and dilute in A. And the third is when both are condensed phases but α is a pure or nearly pure A while β is dilute in A. In any of the three cases, the "invariant" thermodynamic quantities are accessible from the solubility Σ via Eq. (6).

The excess chemical potential of A in a given phase with the number density ρ of A is defined by

$$\mu^{\text{ex}} = \mu(\rho, T) - \mu^{\text{id}}(\rho, T) = -kT \ln(\rho/\zeta), \tag{8}$$

where $\mu^{\text{id}}(\rho, T) = kT \ln \rho\Lambda^3$ is the chemical potential of the ideal gas with the same number density and the same molecular mass and $\zeta = \Lambda^{-3} \exp(\mu/kT)$ is the activity of A; Λ is the de Broglie thermal wavelength. The excess entropy s^{ex} and the excess enthalpy h^{ex} are defined, respectively, by

$$s^{\text{ex}} = s - s^{\text{id}} \tag{9}$$

and

$$h^{\text{ex}} = h - h^{\text{id}} = \mu^{\text{ex}} + Ts^{\text{ex}}, \tag{10}$$

where $s = -(\partial\mu/\partial T)_P$, $s^{id} = -(\partial\mu^{id}/\partial T)_{Pid}$, $h = [\partial(\mu/T)/\partial(1/T)]_P$, and $h^{id} = [\partial(\mu^{id}/T)/\partial(1/T)]_{Pid}$, the temperature differentiations of μ being at fixed pressure P of the real phase and those of μ^{id} being at fixed pressure P^{id} ($\neq P$) of the ideal gas at the same density ρ and temperature T.

In contrast to ΔG^* and its derivatives, the excess quantities are defined by properties of the phase of interest alone, without any reference to a second phase, and they appear more often in theoretical than experimental studies: in general, they are not directly accessible by experiments. The thermodynamic quantities of transfer are, however, related to the excess quantities of the two phases α and β:

$$\Delta G^* = \mu^{\beta,ex} - \mu^{\alpha,ex}, \quad \Delta S^* = s^{\beta,ex} - s^{\alpha,ex},$$
$$\Delta H = h^{\beta,ex} - h^{\alpha,ex}. \tag{11}$$

If α is an ideal gas with an *arbitrary* density of A, the thermodynamic quantities of transfer are identical to the excess quantities

$$\Delta G^* = \mu^{\beta,ex}, \quad \Delta S^* = s^{\beta,ex},$$
$$\Delta H = h^{\beta,ex}. \tag{12}$$

Substituting these and $\epsilon^\alpha = 1/T$ into the general identities, Eqs. (3) and (5), one finds the analogous identities for the excess quantities:

$$s^{ex} = -\frac{\partial\mu^{ex}}{\partial T} + kT(\epsilon - 1/T) \tag{13}$$

and

$$h^{ex} = \frac{\partial\mu^{ex}/T}{\partial 1/T} + kT^2(\epsilon - 1/T), \tag{14}$$

where the temperature differentiations are at fixed pressure of the β phase. Here and below, the superscripts β are omitted unless specification of each phase is necessary. Equations (13) and (14) may be obtained from Eqs. (8), (9), and (10) without referring to any transfer process. Note then that the temperature differentiations of μ^{id} in Eq. (8), too, are to be at fixed P, not P^{id}.

When α is a dilute gas of A, μ^{ex} of the β phase becomes practically identical to ΔG^*, and so accessible from experimental measurements of Σ alone; otherwise μ^{ex} is different from ΔG^*, and so its determination requires μ^{ex} of the other phase in addition to ΔG^*.

Figure 1 shows $\Delta G^*/kT$, $-\Delta S^*/k$, and $\Delta H/kT$ of methane as functions of temperature, which are derived from temperature dependence of Henry's constant evaluated by Fernández Prini and Crovetto.[30] In evaluating ΔG^*, we have chosen an isobar of 0.5 MPa (only because the solvent water, then, remains to be a liquid up to 425 K); the values are essentially the same as those at 0.1 MPa or 1 bar, for Henry's law holds in that pressure range. Also these thermodynamic quantities of transfer are essentially identical to the corresponding excess quantities μ^{ex}/kT, $-s^{ex}/k$, and h^{ex}/kT because the methane gas is ideal in that pressure range. The characteristic features of the hydrophobic hydration are apparent around the room temperature: (i) $\Delta G^*/kT$ increases, so the solubility Σ decreases, with increasing T, (ii) the un-
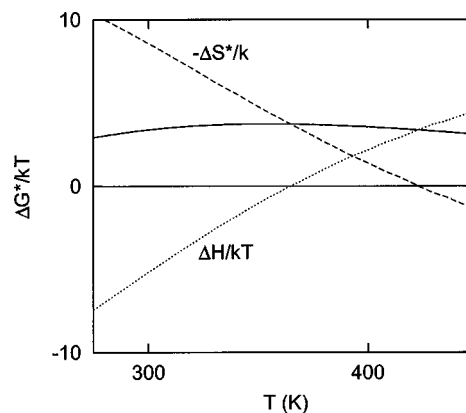

FIG. 1. $\Delta G^*/kT$ (solid curve), $-\Delta S^*/k$ (dashed curve), $\Delta H/kT$ (dotted curve) of methane as functions of temperature T [from solubility data of Fernández-Prini and Crovetto (Ref. 30)]. These are essentially identical to the corresponding excess quantities μ^{ex}/kT, $-s^{ex}/k$, and h^{ex}/kT.

favorable entropic part $-\Delta S^*/k$ overweighs the favorable energetic part $\Delta H/kT$, and (iii) there is considerable cancellation between the entropic and energetic parts. These features disappear around and above 355 K, the temperature of maximum ΔG^* or minimum Σ. At 365 K, $\Delta H/kT = 0$, and so $\Delta G^*/kT$ is entirely $-\Delta S^*/k$ and $\Delta S = 0$. At temperatures between 365 K and 425 K, $-\Delta S^*/k > 0$ and $\Delta H/kT > 0$, i.e., the hydration of methane is unfavorable both entropically and energetically. At 393 K the two contribute equally to the low solubility: $-\Delta S^*/k = \Delta H/kT = (1/2)\Delta G^*/kT$. At 425 K, $\Delta S^*/kT = 0$, or equivalently, $\Delta S/k = -\ln(\rho^\beta/\rho^\alpha)$, and so the low solubility is solely due to the unfavorable enthalpy change: $\Delta G^*/kT = \Delta H/kT$. At temperatures greater than 425 K, what makes the solubility so low ($\Delta G^*/kT$ at 450 K is nearly the same as that at 280 K) is completely different from the mechanism of the hydrophobic effect: it is an unfavorable energy change overweighing a favorable entropy change. Therefore, the temperature of maximum $\Delta G^*/kT$ may be taken to be a characteristic temperature T_1 of solvation, above which the hydrophobic effect is lost.

The hydrophobic attraction is another manifestation of the hydrophobic effect. The (positive) solvation free energy of a pair of solute molecules is less when the two are close together than when they are far apart. This results in an effective solvent-mediated attraction. Let W be the solvent-mediated part of the potential of mean force between a pair of A molecules with a given configuration, μ_d^{ex} be the excess chemical potential for the pair with that configuration, and μ^{ex} be the excess chemical potential of a single A molecule. Then

$$W = \mu_d^{ex} - 2\mu^{ex}. \tag{15}$$

Furthermore, let s_d^{ex} and h_d^{ex} be the excess entropy and the excess enthalpy of the pair of A molecules with that configuration, and define the differences in entropy and enthalpy by

$$\delta s^{ex} = s_d^{ex} - 2s^{ex}, \quad \delta h^{ex} = h_d^{ex} - 2h^{ex}. \tag{16}$$

Then from Eq. (10) and an analogous identity $h_d^{ex} = \mu_d^{ex} + Ts_d^{ex}$ for the pair,

$$W = \delta h^{ex} - T\delta s^{ex}. \tag{17}$$

Substitution of Eqs. (13) and (14) and analogous identities for s_d^{ex} and h_d^{ex} into Eq. (16) and use of Eq. (15) result in

$$\delta s^{\mathrm{ex}} = -\frac{\partial W}{\partial T} - kT(\epsilon - 1/T) \qquad (18)$$

and

$$\delta h^{\mathrm{ex}} = \frac{\partial W/T}{\partial 1/T} - kT^2(\epsilon - 1/T). \qquad (19)$$

These are the analogs of Eqs. (3) and (5) or Eqs. (13) and (14); but the signs of the second terms are opposite to their analogs.

It is difficult to measure W, unlike ΔG^*, by experiments. (And it is true even for a most probable configuration of the pair of A molecules.) But molecular theories and computer simulations support that W at a most probable configuration is negative (the hydrophobic attraction) and $-W$ is of the order of kT.[8,9,11,13,14,17–19,22] Moreover, since the underlaying mechanism of the hydrophobic attraction is the same as that of the hydrophobic hydration it is expected that temperature dependence of $-W/kT$ is similar to that of ΔG^*. That is, one may expect that there is a temperature T_2 at which $-W/kT$ is maximal. At temperatures below T_2, the solvent-mediated attraction results from a favorable entropy difference overweighing an unfavorable enthalpy difference: i.e., $\delta s^{\mathrm{ex}}/k > 0$, $\delta h^{\mathrm{ex}}/kT > 0$, and $\delta s^{\mathrm{ex}}/k - \delta h^{\mathrm{ex}}/kT$ $(= -W/kT) > 0$. At temperatures above the temperature of maximum $-W$, which is even higher than T_2, the solvent-mediated interaction is attractive because a favorable enthalpy difference ($\delta h^{\mathrm{ex}}/kT < 0$) overweighs an unfavorable entropy difference ($\delta s^{\mathrm{ex}}/k < 0$). Therefore one may consider T_2 as another characteristic temperature of the hydrophobic effect.

We are interested in not only T_1 and T_2 for a given system at a given pressure but also their pressure dependences. Let us then ask how much pressure needs to be applied until ΔG^* or μ^{ex} changes significantly. Differentiating Eq. (1) with respect to P at fixed T and fixed composition gives

$$\frac{\partial \Delta G^*}{\partial P} = v_A^\beta - v_A^\alpha - kT(\chi_T^\beta - \chi_T^\alpha), \qquad (20)$$

where v_A^β is the partial molar volume of A in the β phase and χ_T^β is the isothermal compressibility of the β phase, and v_A^α and χ_T^α are those for the α phase. If the α phase is taken to be an ideal gas, then $\Delta G^* = \mu^{\mathrm{ex}}$ and $kT\chi_T^\alpha = v_A^\alpha$ in Eq. (20), and so

$$\frac{\partial \mu^{\mathrm{ex}}}{\partial P} = v_A^\beta - kT\chi_T^\beta. \qquad (21)$$

When the β phase is far from the critical point, $\partial \mu^{\mathrm{ex}}/\partial P \simeq v_A^\beta$, for the second term in Eq. (21) is much smaller than the first. For methane, the partial molar volume at 298 K at infinite dilution in water is 36.17 cm^3 mol^{-1}.[31] This means that the fractional change $(\partial \mu^{\mathrm{ex}}/\partial P)/\mu^{\mathrm{ex}}$ is 4×10^{-4} bar^{-1}; e.g., raising P from 1 bar to 100 bars causes only 4% increase in ΔG^* or μ^{ex}.
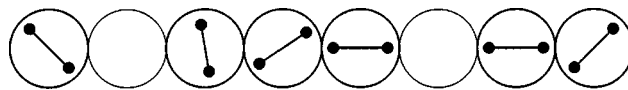

FIG. 2. Schematic picture of the model in one dimension. Each circle with a bar represents a solvent molecule, each open circle represents a cavity formed by two neighboring solvent molecules. Orientation of each bar shows a state of each solvent molecule: the horizontal orientation means the special state and any other orientation means one of $q-1$ nonspecial states. Two neighboring solvent molecules both in the special state interact with each other with energy w and *always* form a cavity (e.g., the fourth and fifth solvent molecules from left), those which are not both in the special state interact with each other with energy 0 if they form a cavity (e.g., the first and second molecules) or u if they do not (e.g., the second and third molecules).

III. MICROSCOPIC MODEL

Our model is an extension of the lattice model of the hydrophobic attraction studied previously.[27–29,32–34] The original model captures the essential mechanism of the hydrophobic hydration in a simplest way, excluding many other realistic features that might obscure results relevant to the hydrophobic effect. The present model is given two additional features: (i) a mechanism of solvation which is different from that of the hydrophobic hydration and becomes dominant with increasing T, and (ii) the pressure as a second thermodynamic field. This is done with the same spirit as the original model in such a way that the model remains simple and exactly soluble in one dimension. The present model is in one dimension but may be extended in any dimensions.

Figure 2 shows a schematic picture of the one-dimensional lattice model. Each cell of volume v_0 may be occupied by a single solvent molecule. Each solvent molecule has q possible states or orientations: one special state (call it 1) and the other $q-1$ states (collectively call them 0). Only neighboring solvent molecules interact with each other. Two neighboring molecules both in state 1 interact with each other with interaction energy $w(<0)$ and form a cavity. One may picture a pair forming a hydrogen bond with open structure. Neighboring molecules that are not both in the special state interact with each other with energy $u(>w)$ if they are in contact with each other and 0 if they form a cavity. The energy u and 0 may be regarded as those of dispersion forces when the pair is in contact with and apart from each other, respectively. The parameters of this model are then $q-1 > 0$, $u-w > 0$, and u. Any single cavity is taken to have the same volume v_0 as that of each cell.

Let N_1, N_0, and N be the number of molecules in the special state, the number of molecules in any other state, and the total number of molecules, respectively; and let N_{11}, N_{01}, and N_{00} be the number of pairs of neighboring molecules both in the special state, the number of neighboring pairs only one of which is in the special state, and the number of neighboring pairs of which neither is in the special state, respectively. Let M be the number of pairs that are not both in the special state *and* have a cavity. Then the total volume V of the system is

$$V = v_0(N + N_{11} + M), \qquad (22)$$

and the total energy of the system of pure solvent is

$$E = wN_{11} + u(N_{01} + N_{00} - M). \tag{23}$$

The isothermal-isobaric partition function is

$$Z(P,T) = \sum e^{-PV/kT} e^{-E/kT}, \tag{24}$$

where the sum runs over all the possible states of the system. Substituting Eqs. (22) and (23) into Eq. (24), summing over $q-1$ energetically equivalent states for each molecule, and summing over all the possible arrangements of cavities for neighboring pairs that are not both in the special state, one obtains

$$Z(\epsilon,T) = e^{-\epsilon N/kT} \sum_{0,1} (q-1)^{N_0} e^{-(w'N_{11} + u'N_{01} + u'N_{00})/kT}, \tag{25}$$

with

$$\epsilon = Pv_0, \quad w' = w + \epsilon, \quad u' = u - kT \ln[1 + e^{-(\epsilon-u)/kT}], \tag{26}$$

where the sum $\Sigma_{0,1}$ runs over two states for each molecule: 1 (the special state) and 0 (a set of the other $q-1$ states). The factor $(q-1)^{N_0}$ is due to the degeneracy $q-1$ for each molecule in state 0. The sum in Eq. (24) is identical to the partition function of the original lattice model,[28] provided that w' and u' are replaced by w and u. The present model is thus equivalent to an Ising spin model or to the corresponding one-component lattice gas as the original and related models.[34,35] Let states 1 and 0 correspond to spins ↑ (the direction of the field) and ↓ in the Ising model. Then the external magnetic field H and the spin-spin interaction energy J in the Ising model are related to $u' - w'$ and $q-1$ by

$$H = \frac{C}{4}(u' - w') - \frac{1}{2} kT \ln(q-1), \quad J = \frac{1}{4}(u' - w'), \tag{27}$$

where C is the coordination number. In one dimension ($C = 2$), the partition function $Z(\epsilon,T)$ is exactly evaluated by the standard transfer matrix method:[36]

$$Z(\epsilon,T) = (e^{-\epsilon/kT} \lambda_1)^N, \tag{28}$$

where

$$\lambda_1 = \frac{1}{2}(q-1)e^{-u'/kT}[x + 1 + \sqrt{X}], \tag{29}$$

with

$$x = \frac{e^{(u'-w')/kT}}{q-1}, \quad y^2 = e^{-(u'-w')/kT},$$

$$X = (x-1)^2 + 4xy^2. \tag{30}$$

Thermodynamic properties of the pure solvent are then obtained by differentiating the Gibbs free energy $G = -kT \ln Z$ or the chemical potential $\mu_w = -kT \ln(e^{-\epsilon/kT} \lambda_1)$ of solvent. The volume per molecule is given by $(\partial \mu_w / \partial p)_T$, which is in a dimensionless form:

$$V^* = \frac{\langle V \rangle}{v_0 N} = 1 + \frac{1}{1+c}\left[1 + \frac{xc}{\sqrt{X}} \cdot \frac{x - 1 + \sqrt{X}}{x + 1 + \sqrt{X}}\right], \tag{31}$$

where

$$c = e^{(\epsilon-u)/kT}. \tag{32}$$

In this model, a solute molecule may be present only between neighboring pairs of solvent molecules, and only then if the pair of solvent molecules has a cavity or an open structure that contributes v_0 to the total volume of the system. A solute molecule in a cavity interacts with the two neighboring solvent molecules with interaction energy v. There are two kinds of cavities: the low-entropy cavity associated with two solvent molecules both in the special state and the high-entropy cavity associated with two solvent molecules that are not both in the special state. Accommodating a solute molecule in the low-entropy cavity forces the two neighboring solvent molecules into the energetically favorable but entropically unfavorable state. This is the essential mechanism of the hydrophobic hydration. But a solute molecule may occupy the high-entropy cavity, too. The low-entropy cavities would prevail if the temperature is low enough, whereas the high-entropy cavities would dominate if the temperature is high enough. In this way the present model may have the temperature T_1 of the solubility minimum as a result of competition between the hydrophobic hydration at $T < T_1$ and the other type of solvation at $T > T_1$.

The ratio ρ/ζ of the number density to the activity of solute in the β phase (solvent) is derived based on the potential distribution theorem,[37] which reads

$$\frac{\rho}{\zeta} = P_c e^{-v/kT} \quad \text{or} \quad \mu^{ex} = -kT \ln(P_c e^{-v/kT}), \tag{33}$$

where P_c is the probability of finding a cavity at any given interstitial site among N such sites between solvent molecules:

$$P_c = \frac{\langle M + N_{11} \rangle}{N} = V^* - 1. \tag{34}$$

Differentiation of Eq. (33) with respect to P at fixed T and fixed composition gives

$$\frac{\partial \mu^{ex}}{\partial P} = kT \chi_T \left(1 + \frac{1}{P_c}\right), \tag{35}$$

where χ_T is the isothermal compressibility of the system,

$$\chi_T = -\frac{1}{V^*}\left(\frac{\partial V^*}{\partial P}\right)_T. \tag{36}$$

An explicit expression for χ_T is given from Eq. (31):

$$\frac{kT V^* \chi_T}{v_0} = \frac{c}{(1+c)^2} + \left(\frac{c}{1+c}\right)^2 \frac{x}{\sqrt{X}}\left(\frac{x - 1 + \sqrt{X}}{x + 1 + \sqrt{X}}\right)$$
$$\times \left[1 - \frac{1}{c} - \frac{x(x-1)}{X} + \frac{2x}{\sqrt{X}(x + 1 + \sqrt{X})}\right]. \tag{37}$$

From the thermodynamic identity (21) and Eq. (35), the partial molar volume of A in the solvent for this model is

$$v_A = kT \chi_T \left(2 + \frac{1}{P_c}\right). \tag{38}$$

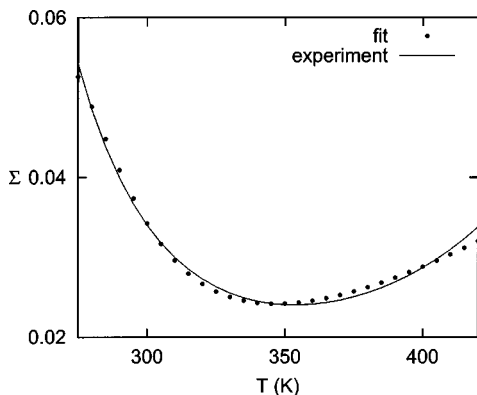J. Chem. Phys., Vol. 121, No. 15, 15 October 2004

Hydrophobic effect   7309

FIG. 3. Fit of the Ostwald coefficient Σ of the one-dimensional model to the experimental Σ for methane. The points are theoretical values with the parameters given in Eq. (39); the curve is from solubility data of Fernandez-Prini and Crovetto (Ref. 30).

FIG. 4. μ^{ex}/kT as a function of T at the six pressures $P = 0.1$, 10, 20, 30, 40, and 50 MPa (from the bottom curve to the top).

To assign realistic values of the parameters in the model solution, we choose a value of v_0 to be fixed at the volume per molecule of liquid water of 1 g/cm^3, and then find values of $q-1$, u, and w to minimize the standard deviation of $T \ln(P_c/\Sigma^{\mathrm{exp}})$ over the temperature range from 275 K to 420 K. The remaining parameter v is given as the average of $kT \ln(P_c/\Sigma^{\mathrm{exp}})$ over that temperature range. Then we obtain the following parameter values:

$$q-1 = 19.64, \quad (u-w)/k = 873.15 \text{ K},$$
$$u/k = -790.00 \text{ K}, \quad v/k = 669.74 \text{ K}. \tag{39}$$

The fit is shown in Fig. 3. It shows that there exists a set of parameter values for the one-dimensional model that gives nearly perfect fit to the experimental Σ over the wide range of temperature including T_1.

Let us now consider the solvent-mediated part $W(r)$ of the potential of mean force between pairs of solutes. We take r to be the number of *solvent molecules* between the two solutes, not a geometrical distance between them. But the geometrical distance, say R, may be defined by the sum of lengths of solvent molecules and lengths of cavities between them, and then for each r at given P and T the average R can be determined. In this model $r=1$ corresponds to the shortest possible distance between two solutes. Let $P(r)$ be the probability that two pairs of solvent molecules, a pair of the ith and $(i+1)$th molecules and a pair of the $(r+i)$th and $(r+i+1)$th molecules, both form a cavity. Then the potential $W(r)$ is given by

$$W(r) = -kT \ln \frac{P(r)}{P_c^2}, \tag{40}$$

where P_c is as defined in Eq. (34). An expression for $P(r)$ is derived as follows. First, for convenience, call a pair of neighboring solvent molecules "special" if both molecules are in the special state. Let then P_{11} be the probability that a single pair of neighboring solvent molecules is special, $P_{11}(r)$ be the probability that two pairs, which are r apart in the same sense as $P(r)$, are both special, $P_{01}(r)$ be the probability that either one of two such pairs is special and the other is not, and $P_{00}(r)$ be the probability that neither is
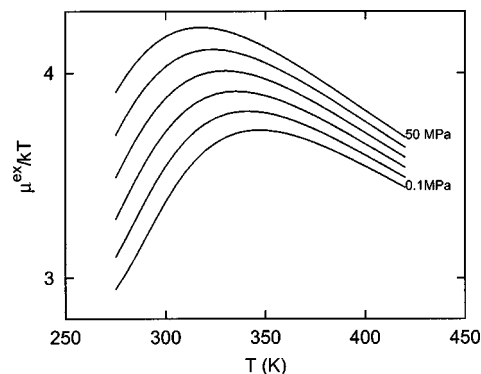
special. These probabilities are all obtained analytically in the one-dimensional model, for they are just the same as the corresponding probabilities in the underlying one-dimensional Ising model with the understanding that a pair of neighboring $\uparrow$ spins is special. The probability $P(r)$ is then given as

$$P(r) = P_{11}(r) + P_{01}(r)P_{\mathrm{cn}} + P_{00}(r)P_{\mathrm{cn}}^2, \tag{41}$$

where P_{cn} is the probability that a cavity be found for any nonspecial pair of solvent molecules, which is given by

$$P_{\mathrm{cn}} = \frac{\langle M \rangle}{N - \langle N_{11} \rangle} = \frac{P_c - P_{11}}{1 - P_{11}}, \tag{42}$$

where M is as defined just above Eq. (22). Two of the three probabilities $P_{11}(r)$, $P_{01}(r)$, and $P_{00}(r)$ in Eq. (41) are expressed in terms of the other and P_{11}: e.g., $P_{01}(r) = 2[P_{11} - P_{11}(r)]$ and $P_{00}(r) = 1 + P_{11}(r) - 2P_{11}$.

IV. HYDROPHOBIC HYDRATION AND HYDROPHOBIC ATTRACTION

Figure 4 shows μ^{ex}/kT as a function of T at the six pressures $P = 0.1$, 10, 20, 30, 40, and 50 MPa. The curve at the lowest pressure is nearly identical to the experimental $-\ln \Sigma$ for methane at the atmospheric pressure, for the model parameters are chosen to fit the experimental data. The figure shows that with increasing P, the whole curve shifts upward; i.e., $(\partial \mu^{\mathrm{ex}}/\partial P)_T \sim v_A^\beta > 0$ at any fixed T in that range, which is consistent with the experimental data for the partial molar volume of nonpolar solutes in water. It is also found that the temperature T_1 of maximum μ^{ex}/kT decreases with increasing P.

Figure 5 shows the partial molar volume v_A of the solute in the solvent as a function of T at the three pressures 0.1, 20, and 50 MPa. We see that the present model, with the parameter values chosen to fit the experimental solubility of methane, gives correct magnitude of v_A for methane at the room temperature.[31] We were unable to find the experimental data on the temperature dependence of v_A for methane; but the results given by this theoretical model seem different from those obtained from experiments for other hydrophobic solutes,[23,25] which indicate near constancy or linear increase of v_A with increasing T. The pressure dependence of v_A at three temperatures 275 K, 325 K, and 375 K is plotted in Fig.
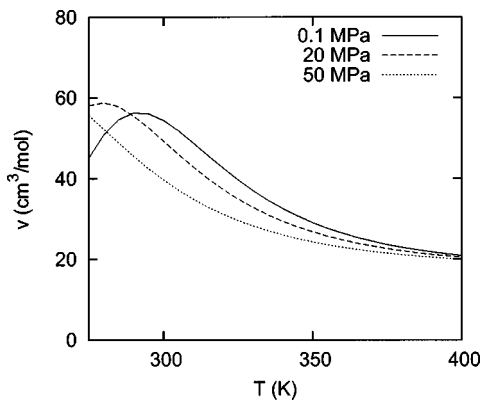
FIG. 5. The partial molar volume v_A as a function of T at the three pressures 0.1, 20, and 50 MPa.

FIG. 7. $-W(1)/kT$ as a function of T at the six pressures $P=0.1$, 10, 20, 30, 40, and 50 MPa (from the bottom curve to the top).

6. The theoretical prediction is qualitatively in good agreement with the experimental result for alkylbenzenes in water:[25] at fixed low temperatures, v_A initially increases and then reaches a maximum with increasing P whereas at fixed high temperatures, it decreases monotonically with increasing P.

The solvent-mediated part $W(1)$ of the potential of mean force between pairs of solutes at $r=1$, divided by kT, is a measure of the strength of hydrophobic attraction. It is plotted in Fig. 7 as a function of T at the six pressures $P=0.1$, 10, 20, 30, 40, and 50 MPa. The strength of attraction as measured by $-W(1)/kT$ shows dependences on temperature and on pressure similar to those of μ^{ex}/kT. At fixed pressures it reaches its maximum, temperature of which is what we call T_2, and then turns to decrease with increasing T; at fixed temperatures (below 350 K) it increases with increasing P, and the characteristic temperature T_2 decreases with increasing P. We note that $W(1)/kT$ represents the solvent-mediated potential of mean force at the shortest possible distance in this model but may not correspond to the one at a contact pair in a real system; computer simulations of methane in water show that strength of solvent-mediated attraction increases with increasing pressure at solvent-separated configurations and at distances shorter than a crossover point around 3.9 Å.[20]

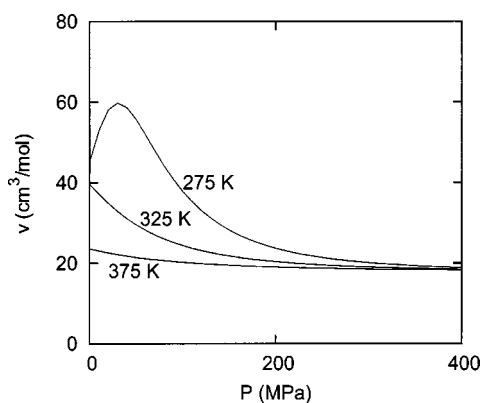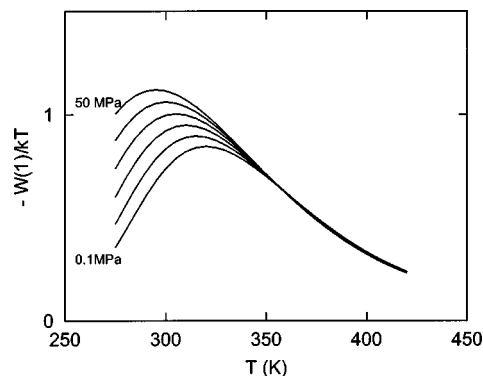The two characteristic temperatures, T_1 and T_2, versus P are plotted in Fig. 8. It shows that T_2 is lower than T_1 at any pressure (e.g., $T_1=347$ K and $T_2=320$ K at 0.1 MPa), suggesting that the hydrophobic attraction becomes strongest at some temperature lower than the temperature of minimum solubility. The figure also shows that the two curves are nearly linear and parallel to each other.

It was found from previous studies of the lattice model that the strength of hydrophobic attraction $-W(1)/kT$ increases nearly linearly with the free energy $\Delta G^*/kT$ of hydrophobic hydration.[27,29] Figure 9 shows the relation between μ^{ex}/kT and $-W(1)/kT$ for the temperature range from 275 K to 350 K at 0.1 MPa. (μ^{ex}/kT is now essentially identical with $\Delta G^*/kT$ because of the low P.) The strength of attraction $-W(1)/kT$ increases with increasing μ^{ex}/kT over a temperature range from 275 K to 320 K, and then turns to decrease. A near linear relation with slight positive curvature does hold over a more restricted temperature range (from 275 K to 310 K $<T_2$), where the hydrophobic effect is dominant over the opposite mechanism of solvation. This model is designed to capture the hydrophobic effect (dominant at low T's) *and* the opposite effect (dominant at high T's) in such a way that a solute may be accommodated in any cavity, whether it is associated with a pair of solvent molecules both in the special states (the low-energy and low-entropy cavity) or it is associated with a pair of solvent molecules that are not both in the special states (the high-energy and high-entropy cavity). Which kinds of cavities are domi-
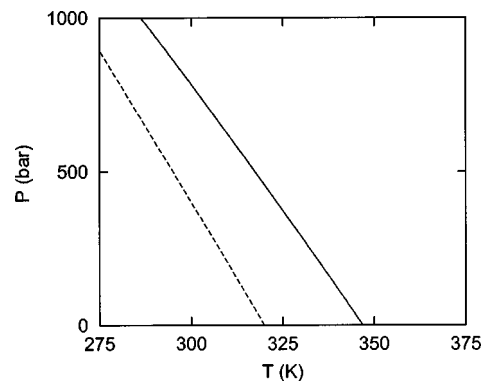

FIG. 6. The partial molar volume v_A as a function of P at three temperatures 275 K, 325 K, and 375 K.

FIG. 8. T_1 vs P (solid curve) and T_2 vs P (dashed curve).

J. Chem. Phys., Vol. 121, No. 15, 15 October 2004
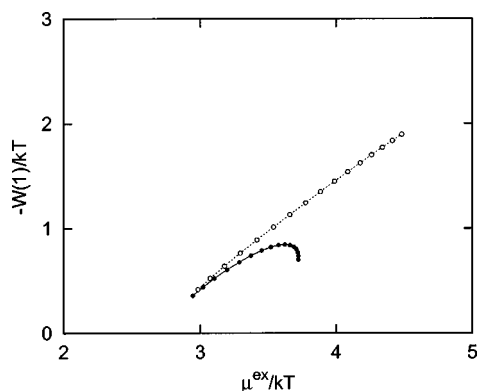
Hydrophobic effect   7311

FIG. 9. μ^{ex}/kT vs $-W(1)/kT$ at 0.1 MPa (solid curve) and the corresponding plot for those associated with the "low-entropy" cavities (dotted curve); see text for the definition. The filled and open dots on the two curves from left to right indicate temperatures from 275, 280,..., to 350 K.

FIG. 10. Plot of sets $[\mu^{ex}/kT, -W(1)/kT]$ at grid points in the area bounded by the curve $T=T_2(P)$ (dashed line in Fig. 7) in the pressure-temperature plane.

nant in the solvent depends on the temperature. It is then possible to extract the hydrophobic effect alone by focusing on the low-energy and low-entropy cavities, i.e., the pairs of solvent molecules both in the special states. That is, we define the free energy μ_0^{ex} of hydration and the solvent-mediated part $W_0(r)$ of the potential of mean force, both associated only with the low-energy and low-entropy cavities:

$$\mu_0^{ex} = -kT\ln(P_{11}e^{-v/kT}), \quad W_0(r) = -kT\ln\frac{P_{11}(r)}{P^2_{11}}. \quad (43)$$

These quantities, too, are analytically obtained in this model. The relation between μ_0^{ex}/kT and $-W_0(1)/kT$ is plotted in the same figure (Fig. 9) as the plot of μ^{ex}/kT versus $-W(1)/kT$. We see a near-perfect linearity, with a slope of 0.99. This result together with the plot of μ^{ex}/kT versus $-W(1)/kT$ suggests that the linear correlation between the free energy of solvation and the strength of solvent-mediated attraction is a characteristic of the hydrophobic effect, and thus eventually disappears at higher temperatures at which the other effect becomes dominant.

To see how far the linear correlation between μ^{ex}/kT and $-W(1)/kT$ holds in the pressure-temperature plane, sets of $[\mu^{ex}/kT, -W(1)/kT]$ are obtained at grid points (with intervals of 0.1 K and 1 MPa) in the restricted region defined by $T \leq T_2(P)$ of the P-T plane, and they are plotted in Fig. 10. We see that all the sets $[\mu^{ex}/kT, -W(1)/kT]$ obtained over the restricted area in the P-T plane fall into a narrow region which is almost a single straight line with a slope near 0.6. As predicted from the previously studied models, the magnitude of $W(1)$ is smaller than that of μ^{ex}: $W(1)$ is only about kT whereas μ^{ex} is about $3kT$ or $4kT$. This result indicates robustness of the linear relation between the free energy of hydrophobic hydration and the strength of hydrophobic attraction: a single, near-linear relation between μ^{ex}/kT and $-W(1)/kT$ holds not only for $T<T_2$ at atmospheric pressure but also for the area, $T \leq T_2(P)$, in the P-T plane where the hydrophobic effect is expected to be dominant over the opposite effect.
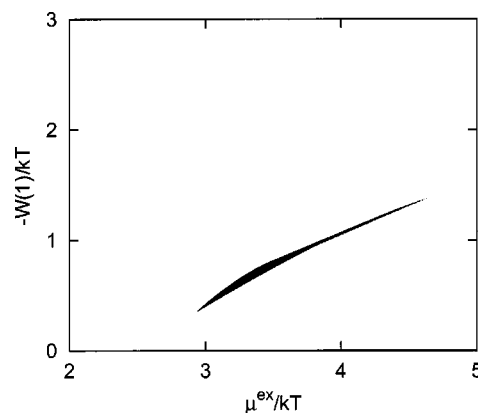
V. SUMMARY

It is remarked in Sec. I that the temperature T_1 of solubility minimum and the temperature T_2 of solvent-mediated attraction maximum are characteristic temperatures of the hydrophobic hydration and the hydrophobic attraction, respectively. The thermodynamics of the hydrophobic effect is outlined in Sec. II. There the thermodynamics of hydration and solvent-mediated attraction is traced from the low-temperature range ($T<T_1$ or $T<T_2$), where the hydrophobic effect manifests itself, to the high temperature range, where the opposite effect dominates. Then a one-dimensional lattice model, an extension of the previously studied model,[28] is proposed with two aims: to capture the solvation and the solvent-mediated attraction of hydrophobic solutes in water in both the low-T and high-T ranges and to consider the effect of pressure in addition to that of temperature. The model parameters were chosen to reproduce the solubility of methane in water over the temperature interval from 275 K to 420 K at a fixed low pressure. It is found that the strength of solvent-mediated attraction measured by $-W(1)/kT$ shows trends qualitatively similar to those of the free energy μ^{ex}/kT of solvation: they initially increase with increasing T but turn to decrease at T_1 or T_2 ($T_1>T_2$); the curve (isobar) of μ^{ex}/kT versus T and that of $-W(1)/kT$ versus T shift upward with increasing P (Figs. 4 and 7); and T_1 and T_2 linearly decrease with increasing P (Fig. 8). While the model seems not to give correct temperature dependence of the partial molar volume of methane in water, the pressure dependences at various temperatures are qualitatively the same as experimental results of hydrocarbons in water. The relation between $-W(1)/kT$ and μ^{ex}/kT is nearly linear at low temperature range but deviates from the linearity as T increases from T_2. On the other hand, the corresponding quantities defined as associated only with the low-energy and low-entropy cavities are linearly correlated with each other over the entire temperature range including T_1 and T_2 (Fig. 9). Finally, the model predicts that the linear relationship is robust in the sense that it holds not only over a temperature range at fixed pressure or over a pressure range at fixed temperature but over a region in the P-T plane where the hydro-

phobic effect is dominant (Fig. 10): such a region is identified as one satisfying $T \leq T_2(P)$ at any given P in the present model.

ACKNOWLEDGMENTS

[1] C. Tanford, *The Hydrophobic Effect: Formation of Micelles and Biological Membranes*, 2nd ed. (Wiley, New York, 1980).
[2] A. Ben-Naim, *Hydrophobic Interactions* (Plenum, Oxford, 1980).
[3] H. S. Frank and M. W. Evans, J. Chem. Phys. **13**, 507 (1945).
[4] W. Kauzmann, Adv. Protein Chem. **14**, 1 (1959).
[5] G. Némethy and H. A. Scheraga, J. Phys. Chem. **66**, 1773 (1962).
[6] G. Némethy, Angew. Chem., Int. Ed. **6**, 195 (1967).
[7] R. L. Baldwin, Proc. Natl. Acad. Sci. U.S.A. **83**, 8069 (1986).
[8] L. R. Pratt and D. Chandler, J. Chem. Phys. **67**, 3683 (1977).
[9] D. E. Smith and A. D. J. Haymet, J. Chem. Phys. **98**, 6445 (1993).
[10] B. Guillot and Y. Guissani, J. Chem. Phys. **99**, 8075 (1993).
[11] S. Garde, G. Hummer, and M. E. Paulaitis, Faraday Discuss. **103**, 125 (1996).
[12] S. Garde, G. Hummer, A. E. García, M. E. Paulaitis, and L. R. Pratt, Phys. Rev. Lett. **77**, 4966 (1996).
[13] G. Hummer, S. Garde, A. E. García, M. E. Paulaitis, and L. R. Pratt, Proc. Natl. Acad. Sci. U.S.A. **95**, 1552 (1998).
[14] S. Garde, A. E. García, L. R. Pratt, and G. Hummer, Biophys. Chem. **78**, 21 (1999).
[15] K. A. T. Silverstein, A. D. J. Haymet, and K. A. Dill, J. Am. Chem. Soc. **120**, 3166 (1998).
[16] G. Graziano, Phys. Chem. Chem. Phys. **1**, 1877 (1999).
[17] N. Matubayasi and M. Nakahara, J. Phys. Chem. B **104**, 10352 (2000).
[18] S. W. Rick, J. Phys. Chem. B **104**, 6884 (2000).
[19] S. Shimizu and H. S. Chan, J. Chem. Phys. **113**, 4683 (2000); **116**, 8636(E) (2002).
[20] T. Ghosh, A. E. García, and S. Garde, J. Am. Chem. Soc. **123**, 10997 (2001).
[21] T. Ghosh, A. E. García, and S. Garde, J. Chem. Phys. **116**, 2480 (2002).
[22] D. Paschek, J. Chem. Phys. **120**, 6674 (2004).
[23] D. R. Biggerstaff and R. H. Wood, J. Phys. Chem. **92**, 1988 (1988).
[24] D. R. Biggerstaff and R. H. Wood, J. Phys. Chem. **92**, 1994 (1988).
[25] S. Sawamura, K. Nagaoka, and T. Machikawa, J. Phys. Chem. B **105**, 2429 (2001).
[26] F. Franks, *Water, A Matrix of Life*, 2nd ed. (Royal Society of Chemistry, Cambridge, 2000).
[27] K. Koga, P. Bhimalapuram, and B. Widom, Mol. Phys. **100**, 3795 (2002).
[28] A. B. Kolomeisky and B. Widom, Faraday Discuss. **112**, 81 (1999).
[29] B. Widom, P. Bhimalapuram, and K. Koga, Phys. Chem. Chem. Phys. **5**, 3085 (2003).
[30] R. Fernández Prini and R. Crovetto, J. Phys. Chem. Ref. Data **18**, 1231 (1989).
[31] A. Ben-Naim, *Solvation Thermodynamics* (Plenum, New York, 1987), Chap. 2, p. 73.
[32] G. T. Barkema and B. Widom, J. Chem. Phys. **113**, 2349 (2000).
[33] D. Bedeaux, G. J. M. Koper, I. Ispolatov, and B. Widom, Physica A **291**, 39 (2001).
[34] G. M. Schütz, I. Ispolatov, G. T. Barkema, and B. Widom, Physica A **291**, 24 (2001).
[35] K. Koga, J. Chem. Phys. **118**, 7973 (2003).
[36] C. Domb, Adv. Phys. **9**, 149 (1960).
[37] B. Widom, J. Chem. Phys. **39**, 2808 (1963).